

# Synthesis of zirconium oxide by hydrolysis of zirconium alkoxide

L. DAVIES\*, L. DAZA†, P. GRANGE

Université Catholique de Louvain, Unité de Catalyse et Chimie des Matériaux Divisés,  
Place Croix du Sud, 2/17, 1348 Louvain-la-Neuve, Belgium

Submicrometre particles have been prepared from hydrolysis-polycondensation of zirconium alkoxide  $[\text{Zr}(n\text{-C}_3\text{H}_7\text{O})_4]$  in ethanolic solution. The properties of these particles (morphology, specific surface area,  $S_{\text{BET}}$ , crystal phase and size distribution) after calcination at 450 °C for 5 h were found to depend on the conditions of synthesis, i.e. alkoxide concentration and mole ratio water/alkoxide.

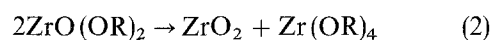
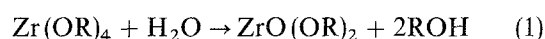
## 1. Introduction

Modern ceramics having a well-defined microstructure are of fundamental importance. The properties of the final product depend on the type and source of raw materials as well as the processing required to prepare these ceramics. In order to improve the properties and reliability of the final product, the microstructure and microstructural uniformity of the green body must be improved. The properties of an idealized sinterable powder for producing a uniform, fully dense, single-phase ceramic at low temperature are believed to be a fine size (between 0.1 and 1  $\mu\text{m}$ ), a narrow size distribution, an equiaxed shape, a non-agglomerate state and high purity. In this way, particle-size distribution is important to achieve maximum particle packing and uniformity so that minimum shrinkage and retained porosity will result during densification. A single particle size does not produce good packing. An optimum packing for spherical particles having all the same size results in over 30% void space [1]. Therefore, to achieve maximum particle packing, a determined and narrow range of particle size is required. Real ceramic particles are generally irregular in shape and do not fit into ideal packing of spheres. So it is desirable to control particle shape and particle-size distribution.

Another important aspect is the reactivity of the starting powder. Reactivity is related to the size and surface area of the particles. Very small particles with high surface areas have a strong thermodynamic driving force to decrease their surface area by bonding together. Particles of 1  $\mu\text{m}$  or less can be compacted and sintered near theoretical density at low temperature. Typically, assuming no microporosity, the finer the powder, the greater the surface area, the lower the temperature and time for densification.

The techniques for synthesizing zirconia powders have been studied by many investigators. Mazdiyasi

*et al.* [2] have investigated the preparation of  $\text{ZrO}_2$  from zirconium alkoxide. They expressed the hydrolysis of zirconium isopropoxide in a simplified form



Bradley and Carter [3, 4] also studied the hydrolysis reaction of some primary zirconium alkoxides. They observed that the hydrolysis of these alkoxides leads to the formation of polymeric oxide-alkoxide  $[\text{ZrO}_x(\text{OR})_{4-2x}]_n$  species.

From these works, it was demonstrated that the hydrolysis behaviour of zirconium alkoxides differs fundamentally from that of silicon, aluminium and titanium alkoxides [5–8]. During hydrolysis, oxo-groups and aqua-groups are formed rather than a true hydroxide. Yoldas [9] has demonstrated that the water-alkoxide ratio in the hydrolysis medium strongly influences the sintering and crystallization behaviour of zirconia powders. In this work, the effect of varying the water-alkoxide ratio and the zirconium alkoxide concentration on the properties and morphology of  $\text{ZrO}_2$ , was studied.

## 2. Experimental procedure

### 2.1. Preparation of samples

$\text{Zr}(n\text{-C}_3\text{H}_7\text{O})_4$  (Fluka) and anhydrous ethanol (Carlo Erba) were used as-received. Zirconium oxide was prepared by controlled hydrolysis of zirconium *n*-propoxide in ethanol. The zirconium alkoxide was diluted with anhydrous ethanol in order to obtain solutions of different concentrations. A predetermined amount of distilled water was also dissolved in anhydrous ethanol and this solution was mixed with the alkoxide solution at room temperature.

The ratio *h*, defined as mole water/mole alkoxide ratio, was varied from 0.5–16. The various *h* values

\* Present address: Universidad Nacional de Salta, Facultad de Ciencias Exactas, Buenos Aires 177, 4400 Salta, República Argentina.

† Present address: Instituto de Catálisis y Petroleoquímica, Campus UAM, Cantoblanco, 28049 Madrid, Spain.

TABLE I Conditions of synthesis. Variation of  $h$  for  $[\text{Zr}] = 0.1 \text{ M}$ 

$h$	Reaction time	Product
0.5	> 1 month	–
1	1 month	–
2	5 min	Sol
4	Instantly	Sol
8	Instantly	Sol
16	Instantly	Sol

TABLE II Conditions of synthesis. Variation of alkoxide concentration for  $h = 2$ 

$[\text{Zr}] (\text{mol l}^{-1})$	Reaction time (min)	Product
0.05	10	Sol
0.1	5	Sol
0.2	1	Sol

studied in this work are listed in Table I. Included also are the times required to observe visually the changes in the solution due to reaction. The concentration of alkoxide was varied from 0.05–0.2 M. Table II lists the values studied for constant  $h$ , i.e.  $h = 2$ . After mixing, the solution turned milky. The time required to observe this reaction is also listed in Table II. Immediately after observing the milky appearance, the solvent was removed in a rotary evaporator. The resulting white powder was dried in air at 120 °C overnight and then calcined at 450 °C for 5 h.

## 2.2. Analysis techniques

### 2.2.1. X-ray diffraction

X-ray diffraction patterns of uncalcined and calcined samples were recorded using a Siemens D5000 diffractometer with  $\text{CuK}\alpha$  radiation. The scans were taken over the range of  $2\theta = 20^\circ\text{--}65^\circ$ . The peaks are due to the (111) diffraction of the metastable tetragonal phase and the (111) and (11–1) diffraction of the stable monoclinic phase.

### 2.2.2. Nitrogen physisorption

Powder surface-area measurements of calcined samples were evaluated by nitrogen (or krypton) adsorption, using an automatic analyser (Micromeritics ASAP 2000). The samples were first outgassed at 130 °C until constant residual pressure had been achieved. Specific surface area was calculated from the BET equation.

### 2.2.3. Particle-size analysis

Particle-size analysis distributions were obtained by light scattering with a Coulter LS 130 instrument which measures particles from 0.1–1000  $\mu\text{m}$ . The equipment employs two systems of measurements. One of them works with light at 750 nm and analyses the particle size from 0.4–1000  $\mu\text{m}$ . The other, the polarization intensity differential scattering (PIDS)

system analyses particles in the 0.1–0.4 mm range and enhances the resolution of the particle size up to 1  $\mu\text{m}$ . It is based on the difference in scattering of vertically versus horizontally polarized monochromatic light at 450, 600 and 900 nm.

Before analysis, the particles need to be dispersed in water. The calcined sample (50–100 mg) was placed in a small beaker with 5  $\text{cm}^3$  water and 2–6 drops of diluted surfactant (1% aqueous solution of sodium pyrophosphate). The beaker was shaken by hand, diluted with 10  $\text{cm}^3$  water and introduced into an ultrasonic bath for 15 min. This was followed by analysis. The optimal amount of sample depends on the powder density (about 6  $\text{g cm}^{-3}$ ), particle size and type of sizing run. The scatter patterns were processed in size (number or volume) distributions using the Fraunhofer model. This model is a simplification of the more rigorous Mie theory. It considers that the particles are spherical and have a smooth surface. The Fraunhofer diffraction theory is also valid when particles are many times larger than the wavelength applied and thus there is no dependence between refractive index and wavelength. In general, it is accepted that a deviation from a spherical shape brings both shifts and broadening in the distribution. When light scattering and PIDS systems are combined with the Fraunhofer theory, accurate and reproducible size-sensitive results can be obtained even for submicrometre samples.

### 2.2.4. Transmission electron microscopy

Transmission electron microscopy (TEM) was used to estimate particle morphology and agglomeration state. Observations were carried in a microscope (Jeol Temscan 100 CX) operating at 100 kV. The TEM samples were prepared by dispersion of the sample in water and depositing a drop on copper grids.

## 3. Results

### 3.1. Variation of the water–alkoxide ratio, $h$

The results obtained when varying the mole ratio  $h$  (mole water/mole alkoxide) are shown in Table I. Under the conditions tested, neither gelation nor precipitation were observed. The reaction time was the time required to observe the change from a clear solution to a milky suspension. The reaction mixture turned milky at different rates depending on the value for  $h$ . For an increase in  $h$ , the rate of reaction increases. For mole ratios below 2, the reaction time was very long.

The dried samples were amorphous to X-ray diffraction. Samples calcined at 450 °C for 5 h crystallized preferentially in the tetragonal phase. This phase is characterized by a peak at  $2\theta = 30.0^\circ$ , which corresponds to the (111) line. Some spectra indicate the presence of a mixture of tetragonal and monoclinic phases. The monoclinic form presents peaks at  $2\theta = 28^\circ$  and  $32^\circ$ , which correspond to the (111) and (11–1) lines.

Fig. 1 shows the XRD diffraction patterns and indicates a decrease of the fraction of the tetragonal phase

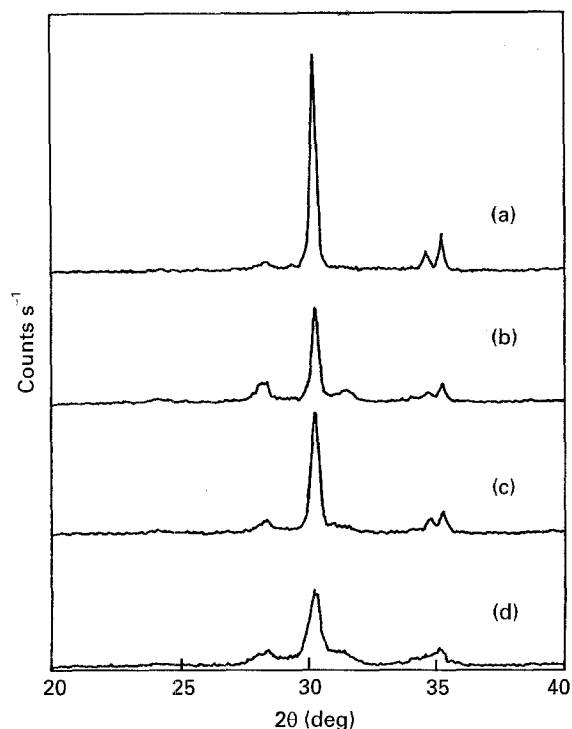


Figure 1 X-ray spectra for calcined samples prepared with  $[Zr] = 0.1$  M and  $h$  (water/alkoxide) variable: (a)  $h = 2$ ; (b)  $h = 4$ ; (c)  $h = 8$ ; (d)  $h = 16$ .

TABLE III Variation of the morphology and texture of zirconia powders calcined at  $450^\circ\text{C}$  for 5 h as function of the mole ratio  $h$  for  $[Zr] = 0.1$  M

$h$	$S_{\text{BET}}$ ( $\text{m}^2 \text{g}^{-1}$ )	TEM
2	11	Spherical
4	26	Unshaped
8	43	Unshaped
16	70	Unshaped

and an increase of the monoclinic phase as a function of mole ratio,  $h$ . A better crystallinity is obtained for samples prepared with lower mole ratios. Table III lists the results of the surface-area measurements and TEM analysis of powders calcined at  $450^\circ\text{C}$ . The surface area,  $S_{\text{BET}}$ , increases with  $h$ . Samples prepared from  $h = 2$  present low  $S_{\text{BET}}$ , about  $10 \text{ m}^2 \text{g}^{-1}$ , while those prepared from  $h = 16$  had an  $S_{\text{BET}}$  of about  $70 \text{ m}^2 \text{g}^{-1}$ . Transmission electron micrographs show that samples prepared from  $h = 2$  were well-defined spherical particles. On the contrary, samples prepared from  $h > 4$  were porous, amorphous (unshaped) agglomerates of very fine particles.

Although the X-ray diffraction,  $S_{\text{BET}}$  and TEM indicate differences between samples prepared from  $h = 2$  and samples prepared from  $h > 4$ , the particle-size analysis by Coulter LS 130 showed no important differences between the samples. The size distributions obtained by this method were broad and contained a variable amount of submicrometre-sized particles which increases with the time of ultrasonic treatment before analysis in addition to a shift in the size distribution to the lowest limit of measurement ( $0.1 \mu\text{m}$ ).

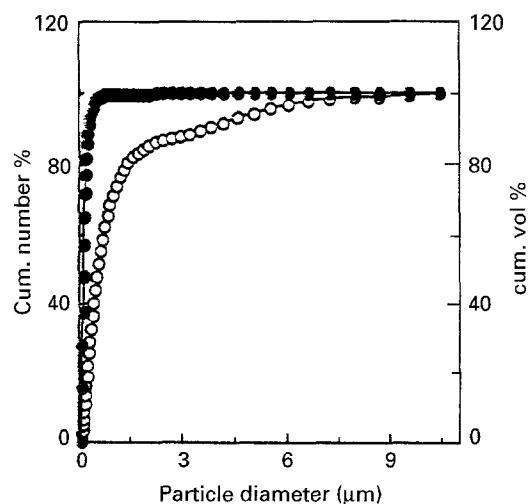


Figure 2 Typical particle size analysis for calcined samples. (●) Number %; (○) Volume %.

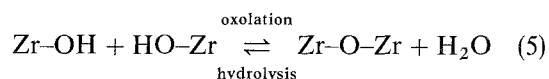
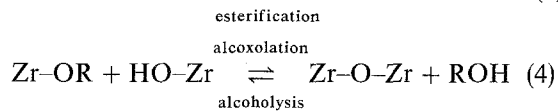
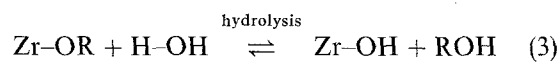
This result indicates the presence of agglomerates which are broken by the ultrasonic waves, giving smaller particles. The results of size distributions were qualitatively confirmed by TEM. Fig. 2 shows a typical size distribution.

### 3.2. Variation of alkoxide concentration

The results of X-ray diffraction,  $S_{\text{BET}}$  and TEM as a function of alkoxide concentration are summarized in Table IV. Fig. 3 shows the X-ray spectra for calcined samples as a function of alkoxide concentration for a mole ratio  $h = 2$ . The monoclinic phase appears at the lowest alkoxide concentration. Surface areas for calcined samples increased when alkoxide concentration decreased. On the other hand, transmission electron micrographs (Fig. 4) showed spherical particles only for samples prepared from 0.1–0.2 M alkoxide.

## 4. Discussion

In ethanolic solution, the zirconium alkoxide is hydrolysed and condensed to form polymeric species composed of M–O–M bonds. The process is generally described schematically as follows



The structure of condensed products depends on the relative rates of these reactions and on external parameters such as mole ratio water/alkoxide and alkoxide concentration.

In an attempt to explain the formation of spherical particles with low  $S_{\text{BET}}$  when  $h = 2$ , we can consider the mechanism of particle formation suggested by Barret and Thomas [10]. Zirconium alkoxide reacts with water to form low molecular weight oligomers,

TABLE IV Properties of zirconia powders calcined at 450 °C for 5 h versus alkoxide concentration for  $h = 2$

[Zr] (mol l <sup>-1</sup> )	$S_{\text{BET}}$ (m <sup>2</sup> g <sup>-1</sup> )	TEM
0.05	19	Unshaped
0.1	11	Spherical
0.2	6	Spherical

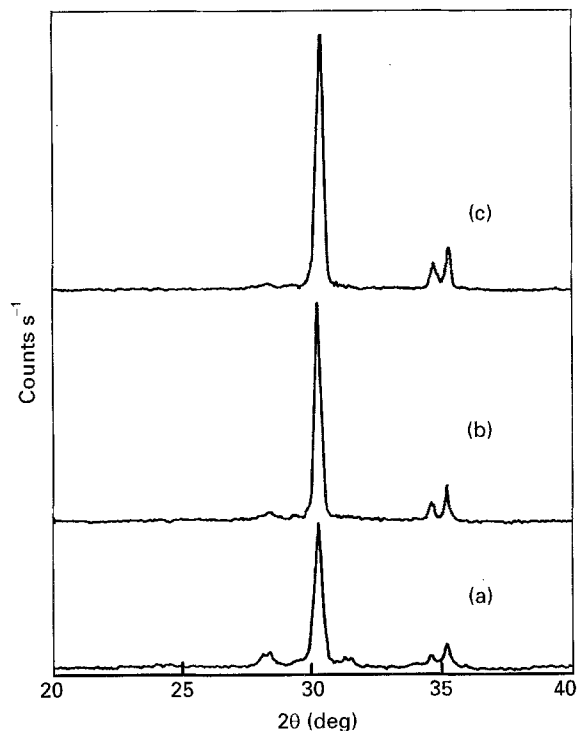


Figure 3 X-ray spectra for calcined samples calcined prepared with  $h = 2$  and [Zr] variable: (a) [Zr] = 0.05 M; (b) [Zr] = 0.1 M; (c) [Zr] = 0.2 M.

which are soluble in ethanol. As the monomer is consumed and the molecular weight of the oligomers increases, the solubility of these oligomers decreases up to a point where they become insoluble. Consequently, zirconium hydrous oxide particles nucleate, the size of these primary particles being in the colloidal range. The period of nucleation and formation of stable colloidal particles is probably short. This leads to a constant number of particles. A constant number of particles is a necessary condition in any model for describing the formation of uniform particles [11]. This is related to the need for colloidal stability, to avoid aggregation or agglomeration. Primary particles or nuclei can absorb free monomer and grow over a longer time to reach a stable final size. The main mechanism of stabilization of these particles is probably due to a hydrogen bond with ethanol rather than electrostatic interactions. The lower dielectric constant of ethanol ( $\epsilon_r = 24.3$ ) compared with water ( $\epsilon_r = 78.5$ ) decreases the importance of electrostatic interactions in this medium [12]. The lower the dielectric constant, the lower the dissociation of ionizable substances. This does not mean that electrostatic interactions are absent. They may arise as

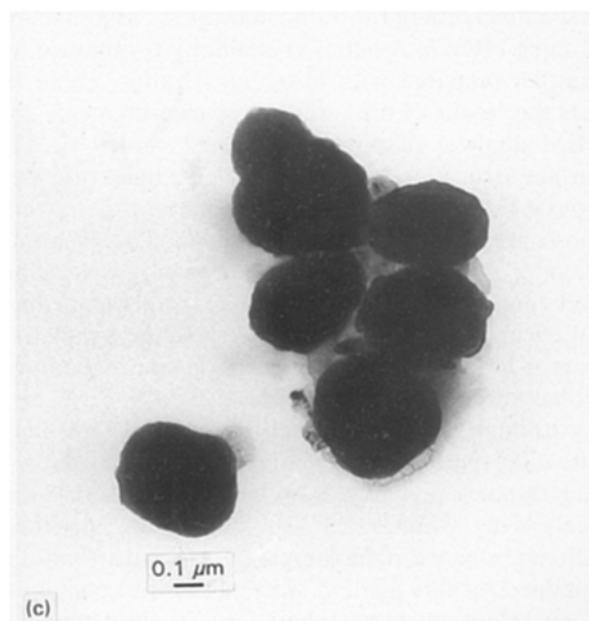
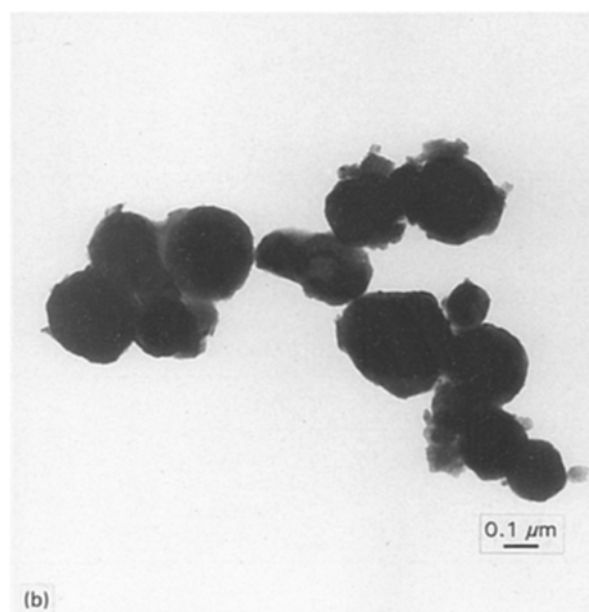
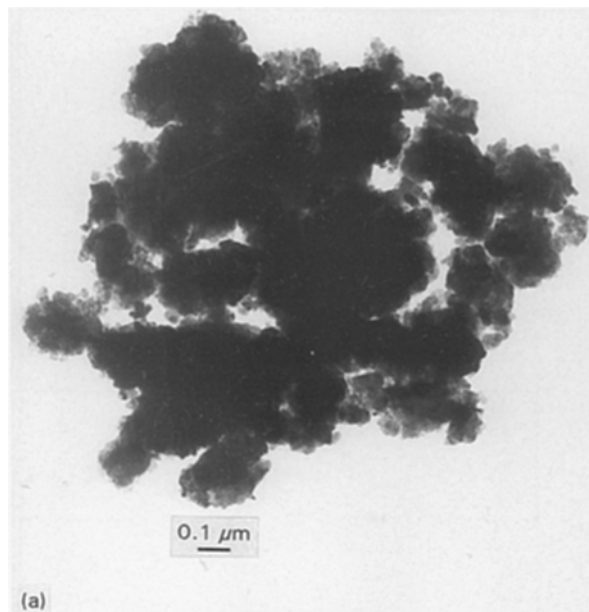


Figure 4 Transmission electron micrographs of calcined samples with  $h = 2$  and [Zr] variable: (a) [Zr] = 0.05 M; (b) [Zr] = 0.1 M; (c) [Zr] = 0.2 M.

an interfacial process of adsorption, surface dissociation and desorption leaving a charge on the particle surface.

This mechanism of particle formation considers that there are two separate steps in the process. The first one, the insolubilization of oligomers leading to a constant number of nuclei, and the second one, the growth of nuclei by adding soluble species. The second step is longer than the first one. A similar model is generally accepted to describe the polymerization of silica in aqueous media [13].

Keefer [14] have demonstrated in computer simulations that condensation is rate-limited, e.g. the probability that any monomer attaches to a nucleus is low with respect to the frequency that it meets a nucleus. Random monomer-cluster aggregation results in smooth uniform particles. This model is based on the supposition that throughout the reaction there is some free monomer available for attachment to a growing particle. This is possible if the rate of hydrolysis (Reaction 3) is slow and if depolymerization (reverse Reactions 4 and 5) occurs to some appreciable extent. So, in our case, for mole ratio  $h = 2$ , the substoichiometric amount of water leads to a slow hydrolysis of alkoxide. Oligomers are formed up to a point where they are insoluble, consequently a solid phase appears at this point. Growth takes place for a longer time by attaching monomer (or soluble species of low molecular weight) to nucleus on the best site, resulting in spherical uniform particles. The capacity for soluble species to select the best site for attachment leads to uniformity in shape of particles and a constant number of nuclei or primary particles leads to uniformity in size. This is confirmed by TEM. Furthermore, the BET area for the sample is about  $10 \text{ m}^2 \text{ g}^{-1}$ , which corresponds to  $0.2 \mu\text{m}$  diameter (calculated from  $D = 6/\rho S_{\text{BET}}$ , with  $\rho = 5.8 \text{ g cm}^{-3}$ ). In addition, the Coulter analysis shows that more than 90% of the particles have a particle size below  $0.5 \mu\text{m}$ .

When that monomer is quickly consumed and the condensation reaction is essentially irreversible [15], a process called reaction-limited cluster-cluster aggregation (RCLA) may take place. Clusters move with Brownian trajectory at velocity inversely proportional to their masses. Clusters attach to other clusters but, due to steric and kinetic constraints, they are unable to fill the space completely. When this occurs, computer simulations indicate that branched structures are obtained [16]. This situation may take place when mole ratio  $h$  is equal to or greater than 4, thus the monomer is fully hydrolysed and consumed in a very short time. Nucleation and growth are not separate steps; growth occurs between clusters resulting in amorphous powders with open structures and higher surface areas (Table III). In this case, a constant number of nuclei is never reached, so there are simultaneously very small and large particles. Small particles are consumed by aggregation to a larger particle, the driving force for this association being the reduction in surface energy. The results for calcined samples prepared from  $h = 4$  show surface areas higher than  $30 \text{ m}^2 \text{ g}^{-1}$ , which indicates porous powders. The particle size calculated from this value is about  $30 \text{ nm}$ ,

which is out of the range of measurement of the Coulter analysis (the lowest limit of measurement is  $0.1 \mu\text{m}$ ). An explanation is the formation of large agglomerates composed of very fine particles. This is confirmed by TEM images: large amorphous agglomerates are composed of very fine particles. In this way, Coulter analysis "sees" these agglomerates as large particles, the result is a broad size distribution.

On the other hand, with a constant mole ratio, i.e.  $h = 2$ , two distinct situations are found. First, when the alkoxide concentration is in the range  $0.1\text{--}0.2 \text{ M}$ , there is a delicate balance between hydrolysis rate and polymerization: nucleation and growth occur as separate steps. Nucleation leads to a constant number of particles. Surface-area measurements indicate a particle size of about  $0.2 \mu\text{m}$  ( $D = 6/\rho S$ ). Number distribution from Coulter analysis agrees well with these values. Second, when alkoxide concentration is lower than  $0.1 \text{ M}$ , the higher dilution produces a larger molecular separation, leading to a change in the growth mechanism. Possibly, the mechanism is no longer reaction-limited but is diffusion-limited (DLA) [17]. Clusters are attached between them irreversibly on first contact, leading to amorphous structures. The results of surface-area measurements, TEM and Coulter analysis confirm the presence of amorphous porous structures. So, dilution plays a role in changing the formation mechanism of these particles, and the final powder is comparable to that prepared from mole ratio  $h > 4$ .

One additional reason for considering a change in the mechanism of particle formation is based on the results of BET areas. When analysing the evolution of surface area with mole ratio  $h$  (Fig. 5) and with alkoxide concentration, a higher slope is observed for the graph  $S_{\text{BET}}$  versus  $h$  than for  $S_{\text{BET}}$  versus alkoxide concentration.

There is another question concerning these results, which is the presence of tetragonal phase at low temperature ( $450^\circ\text{C}$ ). The results show that tetragonal phase appears only when the water/alkoxide ratio equals 2 and alkoxide concentration is between  $0.1$  and  $0.2 \text{ M}$ . This coincides also with low surface area and spherical shape of the powders. Up to now, the factors governing the occurrence of the metastable tetragonal zirconia are still controversial. Several authors have given different explanations, such as effects based on surface energy considerations [18], the presence of impurities or lattice defects [19], structural similarities between the amorphous state and tetragonal phase [20], chemical factors arising from conditions of synthesis [21] and conditions of calcination [22, 23].

It is known that the chemistry of aqueous zirconia solutions is very complex. Positive polyvalent species have been postulated at very low pH [24]. On the contrary, in ethanolic solutions, polynuclear positively charged species may not exist due to the lower dielectric constant of ethanol compared with water, but some neutral polynuclear species exist. These species polymerize in different ways according to the amount of water available. So the crystal phase that appeared

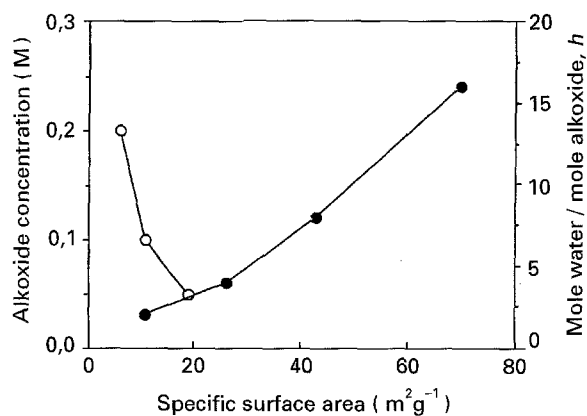


Figure 5 Variation of specific surface area versus water/alkoxide molar ratio,  $h$ , and alkoxide concentration, [Zr].

after calcination may be determined by reaction kinetics that critically depend on water concentration, that is to say,  $h$ . This agrees with what was observed in aqueous pH–time dependent systems [25]. However, further detailed studies are needed to elucidate this point.

## 5. Conclusion

The water–zirconium alkoxide ratio, as well as the alkoxide concentration, are important parameters which control nucleation and growth of zirconium hydrous oxide particles. Homodisperse, submicrometre-size  $ZrO_2$  particles are obtained in a narrow range of experimental conditions. The optimal domain is 0.1 M alkoxide concentration with water/alkoxide molar ratio of 2.

## Acknowledgement

We acknowledge financial support of the “Région Wallonne”, Belgium, through the programme “Multi-matériaux”.

## References

1. D. W. RICHERSON, “Modern ceramic engineering: properties, processing and use in design” (Marcel Dekker, New York, 1992).
2. K. S. MAZDIYASNI, C. T. LYNCH and J. S. SMITH, *J. Am. Ceram. Soc.* **50** (1967) 532.
3. D. C. BRADLEY and D. G. CARTER, *Can. J. Chem.* **39** (1961) 1434.
4. *Idem, ibid.* **40** (1962) 15.
5. B. FEGLEY Jr and E. A. BARRINGER, *Mater. Res. Soc. Symp. Proc.* **32** (1984) 187.
6. B. FEGLEY Jr, P. WHITE and H. K. BOWEN, *Am. Ceram. Soc. Bull.* **64** (1985) 1115.
7. J. LIVAGE, M. HENRY and C. SANCHEZ, *Prog. Solid State Chem.* **18** (1988) 259.
8. J. K. BAILEY and M. L. MECARTNEY, *Mater. Res. Soc. Symp. Proc.* **180** (1990) 153.
9. B. E. YOLDAS, *J. Mater. Sci.* **21** (1986) 1080.
10. K. E. J. BARRET and H. R. THOMAS, in “Dispersion polymerization in organic media”, edited by K. E. J. Barret (Wiley, London, 1975) Ch. 4.
11. C. F. ZUKOSKI, M. K. CHOW, G. H. BOGUSH and J. L. LOOK, *Mater. Res. Soc. Symp. Proc.* **180** (1990) 131.
12. F. N. FOWKES, in *Advances in ceramics*, Vol. 21, “Ceramic powder science”, edited by G.L. Messing, K. S. Mazdiyasi, J. W. McCauley and R. A. Haber (American Ceramic Society, Westerville, OH, 1987) p. 411.
13. R. K. ILER, “The chemistry of silica” (Wiley, New York, 1979).
14. K. D. KEEFER, in “Better ceramics through chemistry II”, edited by C. J. Brinker, D. E. Clark and D. R. Ulrich (Materials Research Society, Pittsburgh, PA, 1986) p. 295.
15. C. J. BRINKER, *J. Non-Cryst. Solids* **100** (1988) 31.
16. C. J. BRINKER and G. W. SCHERER, “Sol-gel science, the physics and chemistry of sol-gel processing” (Academic Press, San Diego, 1990).
17. P. MEAKIN, *Mater. Res. Soc. Symp. Proc.* **180** (1990) 141.
18. R. C. GARVIE, *J. Phys. Chem.* **82** (1978) 218.
19. M. I. OSENDI, J. S. MOYA, C. J. SERNA and J. SORIA, *J. Am. Chem. Soc.* **68** (1985) 135.
20. J. LIVAGE, K. DOI and C. MAZIÉRES, *ibid.* **51** (1968) 349.
21. R. SRINIVASAN, R. DE ANGELIS and B.H. DAVIS, *J. Mater. Sci.* **21** (1986) 583.
22. X. TURRILLAS, P. BARNES, D. HAÜSERMANN, S. L. JONES and C.J. NORMAN, *J. Mater. Res.* **8** (1993) 163.
23. M. A. BLESA, J. G. MAROTO, S. J. PASSAGIO, N. EFIGLIOLA and G. RIGOTTI, *J. Mater. Sci.* **20** (1985) 4601.
24. C. F. BAES, Jr and R.E. MESMER, “The hydrolysis of cations” (Wiley, New York, 1976).
25. R. SRINIVASAN, M. B. HARRIS, S. F. SIMSON, R. J. DE ANGELIS and B. H. DAVIS, *J. Mater. Sci.* **23** (1988) 787.

Received 22 December 1994

and accepted 2 May 1995